Random matrix theory for analyzing the brain functional network in attention deficit hyperactivity disorder

Rong Wang,[1] Li Wang,[2] Yong Yang,[3] Jiajia Li,[1] Ying Wu,[1,*] and Pan Lin[4,5,†]

[1]*State Key Laboratory for Strength and Vibration of Mechanical Structures, School of Aerospace, Xi'an Jiaotong University, Xi'an 710049, China*

[2]*Faculty of Health, Medicine and Life Sciences, Maastricht University, Maastricht, Netherlands*

[3]*School of Information Technology, Jiangxi University of Finance and Economics, Nanchang, China*

[4]*The Key Laboratory of Child Development and Learning Science of the Ministry of Education, Research Center for Learning Science, Southeast University, Sipailou, Nanjing 210096, China*

[5]*Key Laboratory of Biomedical Information Engineering of Education Ministry, Institute of Biomedical Engineering, Xi'an Jiaotong University, Xi'an 710049, China*

(Received 23 June 2016; revised manuscript received 26 September 2016; published 23 November 2016)

Attention deficit hyperactivity disorder (ADHD) is the most common childhood neuropsychiatric disorder and affects approximately 6–7% of children worldwide. Here, we investigate the statistical properties of undirected and directed brain functional networks in ADHD patients based on random matrix theory (RMT), in which the undirected functional connectivity is constructed based on correlation coefficient and the directed functional connectivity is measured based on cross-correlation coefficient and mutual information. We first analyze the functional connectivity and the eigenvalues of the brain functional network. We find that ADHD patients have increased undirected functional connectivity, reflecting a higher degree of linear dependence between regions, and increased directed functional connectivity, indicating stronger causality and more transmission of information among brain regions. More importantly, we explore the randomness of the undirected and directed functional networks using RMT. We find that for ADHD patients, the undirected functional network is more orderly than that for normal subjects, which indicates an abnormal increase in undirected functional connectivity. In addition, we find that the directed functional networks are more random, which reveals greater disorder in causality and more chaotic information flow among brain regions in ADHD patients. Our results not only further confirm the efficacy of RMT in characterizing the intrinsic properties of brain functional networks but also provide insights into the possibilities RMT offers for improving clinical diagnoses and treatment evaluations for ADHD patients.

DOI: 10.1103/PhysRevE.94.052411

I. INTRODUCTION

Attention deficit hyperactivity disorder (ADHD) is one of the most commonly diagnosed neuropsychiatric disorders in children [1]. Clinical diagnosis is based on the fact that children with ADHD exhibit abnormal behaviors of inattention, hyperactivity, and impulsivity [2]. These symptoms cause these children to be more easily distracted, less able to focus on a single task, and constantly in motion and impatient; this not only affects their academic performance and social lives but also places a heavy burden on their families and society [3]. However, the etiology of ADHD is thus far unclear and requires further study.

Recently, a number of studies have focused on investigations of brain functional connectivity based on neuroimaging technologies, such as electroencephalography (EEG), magnetoencephalography (MEG), and functional magnetic resonance imaging (fMRI) [4–6]. Many groups have explored the changes in brain functional connectivity between different brain states, such as the ongoing cognition process [7], the learning experiences [8], and ADHD [9–11]. However, most analyses of functional connectivity in ADHD patients have been based on the Pearson correlation coefficient (CF) between different brain regions [12]. This kind of functional connectivity is linearly dependent and undirected; the advantage of this approach is that it is effective for measuring the synchronization among brain activity signals captured from different brain regions, but it also has the disadvantages that it is not robust to outliers and is unable to reflect any information regarding causality [12,13]. By contrast, the directed functional connectivity is useful for characterizing causality or information transmission between different brain regions. For example, the cross-correlation coefficient (CC) measures linear dependence and causality [14,15], and the mutual information (MI) reflects both linear and nonlinear dependencies and characterizes information transmission across brain regions [13,16]. Both CC and MI reflect directed functional connectivity and take high values when information regarding one region can be used to predict the characteristics of other regions [13]; therefore, these measures better describe the functional causal relationships between brain regions and are more beneficial for further revealing the mechanism of ADHD.

The brain functional network consists of the brain regions and the functional connectivity between them, and this concept has been widely used to explore the various mental states of the brain [3,17–20]. The complex network method is the most commonly used method of characterizing the topological properties of complex networks and has also been proved to be sensitive to the brain functional network in ADHD patients [3,12,20–23]. However, the complex network method cannot capture the intrinsic properties of complex systems,

*Corresponding author: wying36@mail.xjtu.edu.cn

†Corresponding author: linpan@mail.xjtu.edu.cn

such as the universal and system-independent behaviors, that are considered to most efficiently reflect the changes in such systems. By contrast, an eigenvalue-based approach can address this limitation, and many studies have demonstrated that the properties of complex networks can be well characterized in terms of the eigenvalues of the associated adjacency matrix [24]. The eigenvalues of a complex system indicate several basic topological properties of that system [25], and eigenvalue-based approaches have been widely used to explore various complex systems, such as the financial crisis [26,27], the housing market [28], the brain functional network [29], and others [30,31]. More recently, the eigenvalue fluctuations in a complex network that are determined according to random matrix theory (RMT) have received considerable attention because of their efficacy in characterizing the intrinsic behavior of complex networks [24,32,33]. RMT was originally proposed for characterizing the statistical properties of the energy spectrum in a nuclear system [34], and subsequently, it has been widely applied to various real systems, such as the stock market [15,26,28], the atmosphere [35], the biological networks [36–38], the quantum graphs [39], and various other model networks [24,32,40,41]. Recent studies have reported the application of RMT in characterizing brain cognitive states [29,42]. For example, RMT has been used to explore the spectral properties of brain functional networks and has been proved to be effective in detecting the differences between brain systems in the resting state and the visual stimulation state [29,42]. More importantly, it has been demonstrated that RMT not only predicts the universal behavior of the brain functional network but also effectively captures the intrinsic changes in the brain functional network [29,42]. Therefore, using RMT to characterize the spectral properties of the brain functional network in ADHD patients will be beneficial for further revealing the relevant intrinsic abnormalities in the brain.

In this paper, we use CF, CC, and MI to construct the undirected and directed brain functional connectivity based on human fMRI data collected from ADHD patients and normal subjects. First, we explore the functional connectivity distribution and find that ADHD patients have increased undirected and directed functional connectivity among brain regions. Second, we study the global properties of the brain functional network, including the eigenvalue distribution and the largest eigenvalue, and suggest that the value of the largest eigenvalue is greater for ADHD patients. Finally, using RMT, we not only predict the universal behavior of the brain functional network but also provide that ADHD patients exhibit a more orderly undirected brain functional network and a more random directed brain functional network.

II. MATERIALS AND METHODS

A. Subjects and MRI acquisition

fMRI data are collected from the open-access "1000 Functional Connectomes Project" [43] in which resting-state fMRI scans have been released by Milham and Castellanos in December, 2009. These data are acquired at resting state

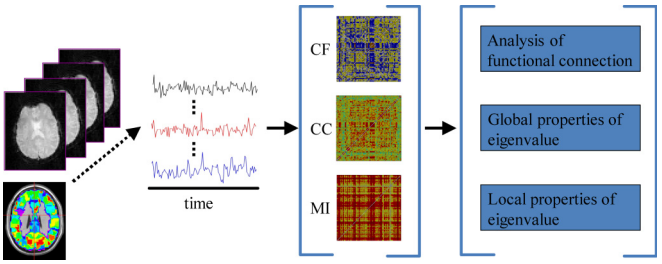

FIG. 1. Flowchart of the methods pipeline: overview of the data processing and analysis pipeline. Resting-state fMRI data were acquired from 24 individual subjects in an ADHD group and a group of 24 healthy controls. Time courses were extracted from the 444 cerebral regions comprising the Multiscale Functional Brain Parcellations template, and the 444 × 444 connectivity matrices were built using CF, CC, and MI. The resulting connectivity matrices were then investigated to identify between-group differences by analyzing the functional connectivity distribution as well as the global and local eigenvalue properties.

by a 3T Siemens scanner. There are 24 ADHD patients in ADHD group, and 24 normal subjects in control group. The voluntary patients in this dataset were evaluated with the clinical interview DSM-IV (SCID), Checklist-90-Revised (SCL-90-R) and Adult ADHD Clinical Diagnostic Scale (ACDS). Image scans contain 39 slices and 192 time points, TR = 2 s, TE = 25 ms, flip angle = 90, matrix = 64 × 64, FOV = 192 mm^2, voxel size = 3 × 3 × 3 mm^3, and the last time is 390 s.

B. fMRI data preprocessing

The AFNI [44,45] and FSL software Library [46] are used to preprocess the functional images, and the first four volumes are excluded from analysis to ensure the initial stabilization of the fMRI signal. For each subject, motion correction is executed through a 3D image realignment with the AFNI program 3dvolreg function, which uses a weighted least squares rigid-body registration algorithm.

Echo planar imaging (EPI) images were motion and slice-time corrected, and spatially smoothed using a Gaussian kernel of 6 mm full width at half maximum (FWHM). The temporal band-pass filtering (0.005 Hz $< f <$ 0.1 Hz) is performed in order to reduce the effects of low-frequency drift and high-frequency physiological noise. After eliminating redundant information of cerebral spinal fluid (CSF) and white matter, fMRI data are further spatially normalized to the Montreal Neurological Institute (MNI) EPI template and resampled to a 3-mm cubic voxel.

C. Construction of the brain functional network

The brain was divided into 444 regions of interest (ROIs) according to the Multiscale Functional Brain Parcellations atlas [47], and the time series for each ROI was obtained by averaging the voxel time series within each ROI. Each brain functional network is represented by a functional connectivity matrix, where the functional connectivity among ROIs was constructed using various methods (see Fig. 1).

1. Pearson's correlation coefficient

The CF serves as the basis of the simplest method of constructing the brain functional connectivity [48], and it is calculated as follows:

$$\rho_{X,Y} = \frac{\sum_{t=1}^{N}(X(t)-\overline{X})(Y(t)-\overline{Y})}{\sqrt{\sum_{t=1}^{N}(X(t)-\overline{X})^2 \sum_{t=1}^{N}(Y(t)-\overline{Y})^2}}, \quad (1)$$

where t stands for the time point, N represents the total number of time points, X and Y are the fMRI time series for different ROIs, and $\overline{X}$ and $\overline{Y}$ are the average values corresponding to these time series. The CF characterizes the linear correlation between different brain regions and reflects the undirected functional connectivity.

2. Cross-correlation coefficient

The CC is used to characterize the directed functional connectivity and measures the causality between different brain regions. A CC is defined as follows [17]:

$$\rho^{m}_{X,Y} = \max_{\tau}\left\{\left|\frac{\xi(X,Y)(\tau)}{\sqrt{\xi(X,X)(0)\xi(Y,Y)(0)}}\right|\right\}, \quad (2)$$

with

$$\xi(X,Y)(\tau) = \begin{cases} \sum_{t=1}^{N-\tau} X(t+\tau)Y(t) & \text{for } \tau > 0, \\ \xi(Y,X)(-\tau) & \text{for } \tau \leqslant 0, \end{cases} \quad (3)$$

where τ is the lag of time point and satisfies $\tau = 0, \pm 1, \pm 2, \ldots, \pm(N-1)$. This algorithm always ensures the strongest directed causality from brain region X to brain region Y or from Y to X with the optimal time lag. The CC-based functional connectivity is linearly dependent but directed, and it measures how one brain region induces changes in the brain activity in another region.

3. Mutual information

The MI also can be used to construct a measure of the functional connectivity. Unlike CF and CC, MI is not limited to real-valued random variables and is a more general means of characterizing the communication of information among brain regions [13]. The normalized MI is calculated as follows [49]:

$$U(X,Y) = 2\frac{I(X,Y)}{I(X)+I(Y)}, \quad (4)$$

with

$$I(X) = -\sum_{x\in X} p(x)\ln p(x),$$
$$I(Y) = -\sum_{y\in Y} p(y)\ln p(y), \quad (5)$$
$$I(X,Y) = \sum_{x\in X}\sum_{y\in Y} p(x,y)\ln\frac{p(x,y)}{p(x)p(y)},$$

where x and y are the random events of X and Y, the $p(x)$ and $p(y)$ are the corresponding probability functions, and the $p(x,y)$ is the joint probability distribution. The MI reflects how the information flows from one brain region to another, and the corresponding MI functional connectivity contains directional information.

After the CF, CC, and MI functional connectivity matrices were constructed, the diagonal elements were all set to zero to eliminate the self-correlation for each ROI, and then a Fisher's r-to-z transformation was applied to improve the normalities of CF, CC, and MI [50]. It should be noted that the CF, CC, and MI functional networks are all undirected even though the CC and MI functional connectivities contain the directional information, which is essential to the application of RMT underlying the real eigenvalues.

D. Random matrix theory

Random matrix theory (RMT) studies the spectral fluctuations in a complex system by separating the system-dependent properties from the random universal component [15,32,41,42]. To analyze the functional networks using RMT, we first need to define a network ensemble. Here, we assume the statistically insignificant difference between the functional networks in each group, and these similar functional networks will represent the network ensemble that we will discuss below.

In RMT, the eigenvalues $\lambda_i (i = 1,2,\ldots,M)$ must first be unfolded through a transformation $\eta_i = F(\lambda_i)$, where $F(\lambda_i) = \int_{\lambda_{min}}^{\lambda_i} \rho(\lambda')d\lambda'$ is the average integrated eigenvalue density of the eigenvalues λ_i and η_i is the unfolded eigenvalue. Because the analytical form of function F is unknown, the unfolding process is performed with the assistance of numerical curve fitting [24,51]. After the unfolding process, the probability density of the unfolded eigenvalues is $\rho(\eta_i) = 1$, which ensures that all eigenvalues are on the same footing and independent of the system. Obviously, the unfolding process removes any spurious effects caused by variations in spectral density [42], and thus, we obtain the more universal properties of the spectral fluctuations. Consequently, we can characterize the changes in the intrinsic behaviors of functional networks that are only related to the ADHD rather than the complex brain system itself.

Using the unfolded eigenvalues, we can calculate the statistical indexes in RMT, such as the nearest-neighbor spacing distribution (NNSD), the spectral rigidity, and number variance. The NNSD is calculated as follows:

$$s_1^{(i)} = \eta_{i+1} - \eta_i, \quad (6)$$

where the unfolded eigenvalues η are ordered such that $\eta_i \leqslant \eta_{i+1}$. The NNSD measures whether an eigenvalue is correlated with its nearest neighbor and reflects only the short-range correlations among eigenvalues [24,51]. If the eigenvalues are uncorrelated, the NNSD follows Poisson statistics and the probability density function satisfies $P(s_1) = \exp(-s_1)$. Otherwise, for correlated eigenvalues, it obeys Gaussian orthogonal ensemble (GOE) statistics and $P(s_1)$ satisfies

$$P(s_1) = \frac{\pi}{2}s_1\exp\left(-\frac{\pi s_1^2}{4}\right). \quad (7)$$

By contrast, the spectral rigidity characterizes the long-range correlations among eigenvalues [52]. For a given unfolded eigenvalue interval $[\eta,\eta+L]$ where the L is the size of the spectral window, the spectral staircase function $f(\eta)$

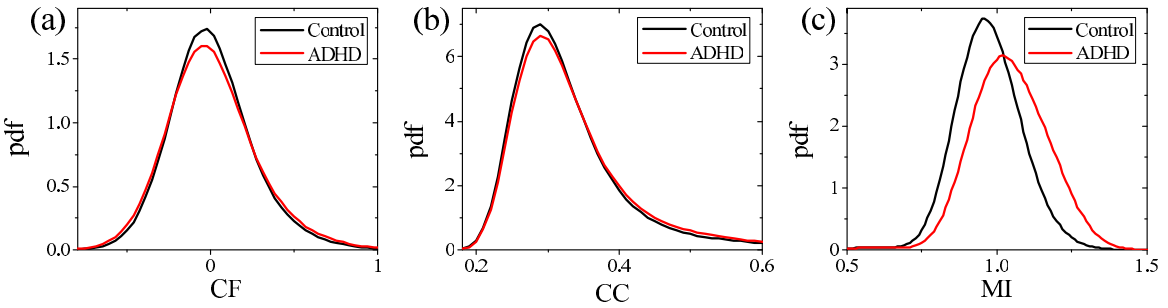

FIG. 2. An analysis of functional connectivity, in which the undirected functional connectivity is measured by CF and the directed functional connectivity is measured by CC and MI. The pdfs of the (a) CF, (b) CC, and (c) MI were calculated individually for the control group and the ADHD group.

representing the cumulative probability of the eigenvalues is deviated from its best straight-line fitting, and the corresponding least-squares deviation is regarded as the spectral rigidity [24,51]:

$$\Delta_3(L;\eta) = \frac{1}{L}\min_{a,b}\int_{\eta}^{\eta+L}[f(\eta') - a\eta' - b]^2 d\eta', \qquad (8)$$

where a and b are the coefficients of the linear equation obtained from a least-squares fit. In the Poisson case, $\Delta_3(L)$ can be predicted by $\Delta_3(L) = \frac{1}{L}$, whereas in the GOE case, $\Delta_3(L)$ depends logarithmically on L:

$$\Delta_3(L) \sim \frac{1}{\pi^2}\ln L. \qquad (9)$$

In addition to the spectral rigidity, the number variance also characterizes the long-range correlations among eigenvalues. The expected number of spectra lying in the interval $[\eta, \eta + L]$ is L and the true number is $E(\eta + L) - E(\eta)$, where $E(\eta) = |\{i \mid \eta_i < \eta\}|$ for the ordered eigenvalue sequence $\eta_1 \leqslant \eta_2 \leqslant, \ldots, \leqslant \eta_M$. The number variance $\Sigma^2(L)$ measures the variance between the expected number and the true number and considers the correlations among consecutive eigenvalues over a length L:

$$\Sigma^2(\eta, L) = \langle (E(\eta + L) - E(\eta) - L)^2 \rangle. \qquad (10)$$

Here, the final number variance $\Sigma^2(L)$ is obtained by calculating the local average $\langle\rangle$ over all chosen η. The value of $\Sigma^2(L)$ for Poisson statistics is $\Sigma^2(L) = L$, and for GOE statistics, $\Sigma^2(L) = \frac{2}{\pi^2}(\ln(2\pi L) + 1.5772 - \frac{\pi^2}{8}) + O(L^{-1})$, where $O(L^{-1})$ is an infinitesimal term and is slightly changed to adapt to the complex system [42,53].

III. RESULTS

A. Analysis of the functional connectivity

In this section, we compare the functional connectivity in the control group and the ADHD group. We first investigate how the undirected functional connectivity measured by the CF is modified by ADHD. Figure 2(a) shows the probability density functions (pdfs) of the CF for the control group and the ADHD group. It is observed that the CF distributions in the different groups are similar; the probability distributions are close to Gaussian statistics. However, the pdf of the CF for the ADHD group is flatted, which reflects an increased CF functional connectivity among brain regions in the ADHD group. To further confirm the difference between the two groups, we performed a statistical Kolmogorov-Smirnov test and provided the statistical difference between the undirected functional connectivity in the control group and the ADHD group ($p < 0.05$). In addition, we explored the directed functional connectivity measured by the CC and MI. Figures 2(b) and 2(c) display the pdfs of the CC and MI for the control group and the ADHD group, respectively. The CC and MI pdfs for the ADHD group are again similar to those for the control group, but both pdfs are shifted toward larger CC and MI values, suggesting increased CC and MI functional connectivity. Furthermore, using the Kolmogorov-Smirnov test, we provided a significant difference between the directed functional connectivity in the control group and that in the ADHD group ($p < 0.05$ for both the CC and MI

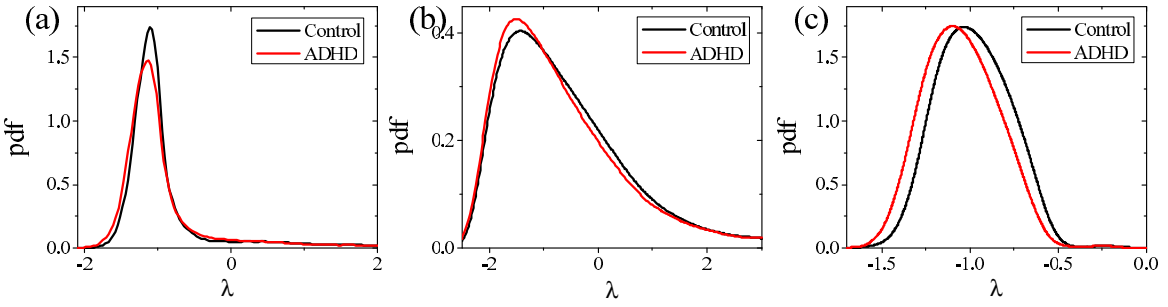

FIG. 3. Global eigenvalue property analysis: the eigenvalue distribution. The eigenvalues were first calculated from the (a) CF, (b) CC, and (c) MI functional networks for the control group and the ADHD group, and the pdfs of the eigenvalues were then calculated.

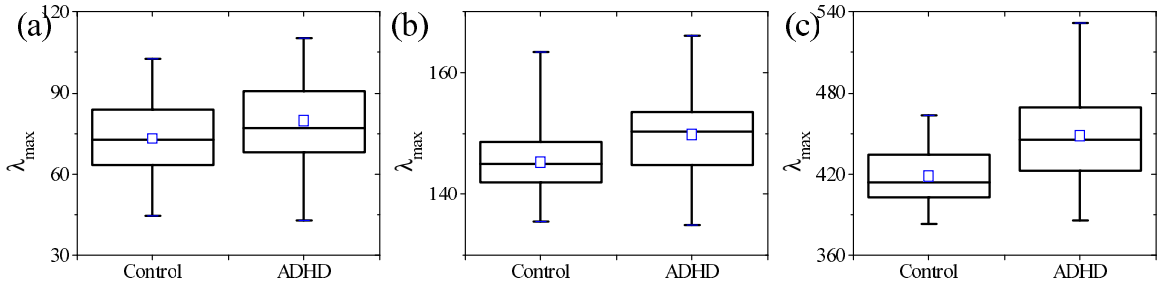

FIG. 4. Global eigenvalue property analysis: the largest eigenvalue. The largest eigenvalues of the brain functional network were first calculated for each subject, and the box plots in each group were then plotted for the (a) CF, (b) CC, and (c) MI functional networks, individually. In the box plot, the bottom and top of the box are the first and third quartiles, the band inside the box is the median, the ends of the whiskers are the minimum and maximum values, and the □ is the mean value.

functional connectivity). Taken together, the results obtained in the functional connectivity analysis suggest the increased undirected and directed functional connectivity in the ADHD group, which reflects the more dense functional networks.

B. Global properties of the eigenvalues

Now, we investigate the global spectral properties of the brain functional network in the control group and the ADHD group. In Figs. 3(a)–3(c), we present the probability distributions of the eigenvalues of the CF, CC, and MI functional networks in both groups. It appears that the distributions of the eigenvalues for the ADHD group are shifted toward smaller eigenvalues for the CF, CC, and MI functional networks. Meanwhile, we performed a Kolmogorov-Smirnov test and found that the differences between the structures of the eigenvalues in the control group and the ADHD group are statistically significant ($p < 0.05$ for the CF, CC, and MI functional networks). These results indicate that ADHD pushes the pdf of the eigenvalues toward smaller eigenvalues, thereby changing the eigenvalue structure in both the undirected and directed functional networks.

Furthermore, we calculated the largest eigenvalue to investigate the differences in the brain functional network between the control group and the ADHD group. Figure 4 shows a comparison of the mean largest eigenvalue in the control group and the ADHD group. As seen from this figure, the mean largest eigenvalue of the brain functional network in the ADHD group is statistically bigger than that in the control group ($p < 0.05$ for the CF, CC, and MI functional networks, two-sample T test). The result indicates that the largest eigenvalue is a significant measure of the changes in the brain functional network caused by ADHD and that ADHD induces an increase in the largest eigenvalues in the CF, CC. and MI brain functional networks.

In summary, we showed a consistent change in the global spectral properties of the undirected and directed functional networks caused by ADHD and provided that ADHD results in changes to the eigenvalue structure and an increase in the largest eigenvalue.

C. Local properties of the eigenvalues

We have found that the functional connectivity and the global properties of the eigenvalues are sensitive to ADHD and that the ADHD-dependent changes in these properties are consistent among the CF, CC, and MI functional networks. To assess the local properties of the eigenvalues, we calculated the spectral fluctuation using RMT. The spectral fluctuation reflects the correlations among eigenvalues: short-range correlations or long-range correlations. The short-range correlation is measured by the NNSD, and the long-range correlation is characterized in terms of the spectral rigidity and number variance.

1. Short-range correlations among eigenvalues

We first investigated whether the short-range correlations among the eigenvalues in the undirected and directed

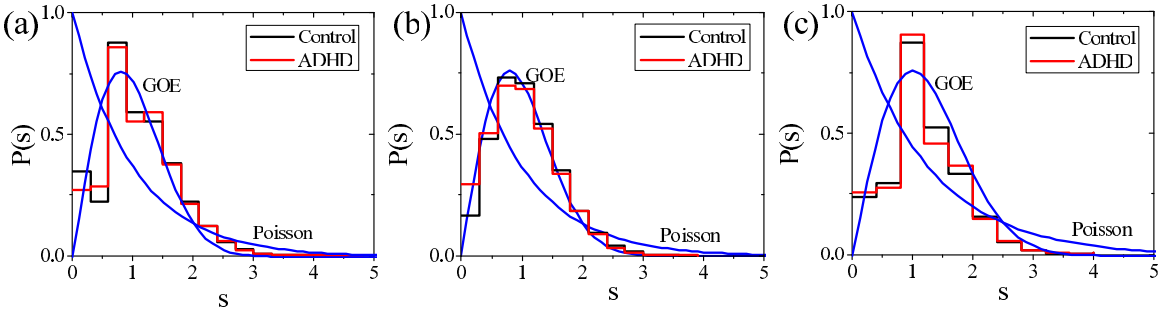

FIG. 5. Local eigenvalue property analysis: the short-range correlations among eigenvalues measured by the NNSD. The NNSD were first calculated for each subject, and the probability distributions were then obtained for each group. The probability distributions of the NNSD for the two groups are plotted separately for the (a) CF, (b) CC, and (c) MI functional networks, where the blue lines represent the empirical values predicted by GOE and Poisson statistics.

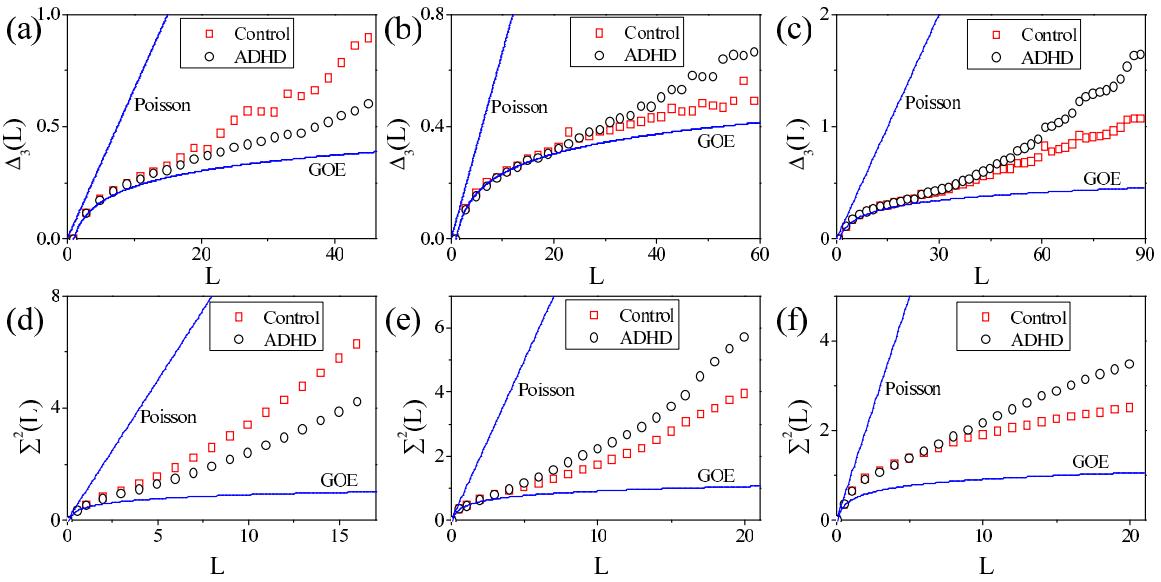

FIG. 6. Local eigenvalue property analysis: long-range correlations among eigenvalues measured by the spectral rigidity and number variance. The spectral rigidity (upper panel) and number variance (lower panel) were first calculated for each subject and then averaged over each group. The mean spectral rigidity and number variance for the two groups are plotted individually for the (a) and (d) CF, (b) and (e) CC, and (c) and (f) MI functional networks. The blue lines represent the empirical values predicted by GOE and Poisson statistics.

functional networks are influenced by ADHD. Figure 5 reports the probability distributions of the NNSD and the values predicted by GOE and Poisson statistics. As seen from this figure, the NNSD distributions in the control group and the ADHD group are closer to GOE statistics than to Poisson statistics in the CF, CC, and MI functional networks, which reflects a large extent of correlation among eigenvalues. Furthermore, it can be observed that the NNSD values in the ADHD group are nearly identical to those in the control group, and this indistinguishability is statistically supported by the Kolmogorov-Smirnov test ($p > 0.05$ for the CF, CC, and MI functional networks). Therefore, this result indicates that the NNSD is unable to reflect the abnormalities in the undirected and directed functional networks induced by ADHD.

2. *Long-range correlations among eigenvalues*

To verity the efficacy of using the long-range correlations among eigenvalues to detect the changes in the brain functional network caused by ADHD, we investigated the spectral rigidity of the brain functional network in the control group and the ADHD group. Figures 6(a)–6(c) show the spectral rigidity in the CF, CC, and MI functional networks for both groups as well as the empirical values predicted by GOE and Poisson statistics. It can be seen that the spectral rigidity values in both groups are in agreement with the GOE predictions for a long range of L in each case ($L \leqslant 11$ for the CF functional network, $L \leqslant 21$ for the CC functional network, and $L \leqslant 25$ for the MI functional network), reflecting the predictable universal properties of the brain functional network. As L increases, the spectral rigidity in both groups becomes increasingly larger than the GOE values, but they remain equal among the CF, CC, and MI functional networks. This phenomenon reflects the intrinsic, specific properties of the brain functional network that not only differ from those of the GOE model but also are unaffected by ADHD. More importantly, a significant difference in spectral rigidity between the control group and the ADHD group appears for sufficiently large L ($L \geqslant 23$ for the CF functional network, $L \geqslant 35$ for the CC functional network, and $L \geqslant 49$ for the MI functional network). For the CF functional network, the spectral rigidity in the ADHD group is significantly smaller than that in the control group [see Fig. 6(a)]. By contrast, the spectral rigidity in the ADHD group is larger than that in the control group for the CC and MI functional networks, as seen in Figs. 6(b) and 6(c). This opposite change in the spectral rigidity strongly indicates that the changes to the brain functional network caused by ADHD are distinct with regard to directed and undirected functional connectivity.

In parallel, we also studied the number variance in the control group and the ADHD group. Despite the similar roles played by the spectral rigidity and number variance in characterizing the long-range correlations among eigenvalues, the algorithms used to calculate them are entirely different. Figures 6(d)–6(f) show the number variances in the control group and the ADHD group and the values predicted by GOE and Poisson statistics. The number variances for both groups agree well with the GOE-predicted values at small L ($L \leqslant 2$ for the CF functional network, $L \leqslant 4$ for the CC functional network, and $L \leqslant 1$ for the MI functional network), reflecting the universal behavior of the brain functional network. As L increases, the number variance deviates from the predicted values, but no differences appear between the two groups, reflecting the intrinsic and specific properties of the brain functional network that are robust to ADHD. When L increases to a sufficiently large value ($L \geqslant 5$ for the CF functional network, $L \geqslant 6$ for the CC functional network, and $L \geqslant 9$ for the MI functional network), a noticeable difference between the number variances for the control group and the ADHD group arises. The number variance for the ADHD group is smaller than that for the control group in the CF

functional network, as seen from Fig. 6(d). However, in the CC and MI functional networks, the number variances for the ADHD group are larger than those for the control group [see Figs. 6(e) and 6(f)]. These results suggest that the number variance is an effective means of revealing the specific changes to the undirected and directed functional networks caused by ADHD.

A comparison of the results presented in Figs. 6(a)–6(c) and 6(d)–6(f) reveals that three different sets of features of the brain functional network appear as both the spectral rigidity and number variance grow with increasing L: universal network behavior is observed at small L, intrinsic and specific properties of the brain functional network that are insensitive to ADHD manifest at larger L, and specific changes related to ADHD emerge at a sufficiently large value of L. Therefore, the spectral rigidity and number variance not only are reliable predictors of the universal behavior of the brain functional network but also are effective in characterizing the intrinsic changes to the brain functional network caused by ADHD.

IV. DISCUSSION AND CONCLUSION

In this study, we characterized both undirected and directed brain functional connectivity using CF, CC, and MI, and we investigated the probability distributions of functional connectivity and the spectral properties of functional networks to understand how ADHD changes the intrinsic properties of the brain functional network. We first found that the functional connectivity indicated by CF, CC, and MI were all significantly increased in the ADHD group compared with the control group. Then, we observed changes in the eigenvalue structure and an increase in the largest eigenvalue related to ADHD. Finally, using RMT, we showed the inability of the NNSD to characterize ADHD-induced changes in the brain functional network and provided that the long-range correlations among eigenvalues measured by the spectral rigidity and number variance not only predict the universal behavior of the brain functional network but also reliably reflect the specific changes to the undirected and directed brain functional networks caused by ADHD.

A. Functional connectivity increase in ADHD patients

Functional connectivity measures the relationship between recorded signals of spatially remote neurophysiological events [54]. This relationship may be either directed or undirected and either linear or nonlinear [13,55]. The CF serves as the traditional means of assessing linear correlation and is used to construct the undirected functional connectivity [48]. The CC represents linear cross correlation and is used to construct a measure of directed functional connectivity [14,56], and the MI characterizes both linear and nonlinear dependence and is also applied as a measure of directed functional connectivity [13,57]. Our results show that ADHD patients exhibit increased functional connectivity as indicated by CF, CC, and MI, which reflects an abnormally coherence among neural activities in different brain regions. Moreover, the CF measures temporal correlation, the CC measures causality, and the MI measures the transmission of information across brain regions [13,57]. The increased functional connectivity observed in the ADHD group reveals a higher degree of linear dependence, stronger causality, and more transmission of information across brain regions. Clinical diagnoses reveal that ADHD patients exhibit hyperactive behavior in the resting state [58], which must be related to certain abnormalities in various regions of the brain and the interactions among them [21,59]. These abnormalities strengthen the information transmission among different regions as well as the causality between them.

More importantly, the increased functional connectivity observed in the ADHD group also reflects higher synchronization of the brain functional network. Previous studies have proved that strong synchronization among neural activities often occurs in pathological scenarios [60], such as epileptic seizures [61], but the brain functional network in cognitive states exhibits decreased functional connectivity and desynchronizing behavior [29]. Our results further provide that strong synchronization occurs in ADHD patients, which may act in opposition to the desynchronization often caused by disease states and may be the origin of the inattentive behavior that is characteristic of ADHD patients.

B. Global eigenvalue properties are sensitive to ADHD

The eigenvalues of the brain functional network reflect the contributions of brain regions to this network in the brain system, and the largest eigenvalue characterizes the principal component of the network and contains the most information [62]. The eigenvalue distribution and the largest eigenvalue have been widely used to characterize changes in various complex systems, such as the financial crisis [26,27], the housing market [28], and the brain functional network [29,42]. Here, the eigenvalue distribution and the largest eigenvalue were used to distinguish the changes to the brain functional network caused by ADHD. Our results show that the eigenvalue structure in the ADHD group is changed with respect to the control group and that the largest eigenvalue is increased in the CF, CC, and MI functional networks. The increased largest eigenvalues observed in the ADHD patients in the resting state reveal that the brain functional network in these patients has higher information energy that needs to be provided by the stronger coupling between brain regions. Therefore, ADHD patients exhibit stronger synchronization of the brain functional network than normal subjects, as shown in Sec. IV A. More importantly, our results indicate that the strong synchronization that occurs in ADHD patients makes the brain functional network resistant to the desynchronization caused by disease states.

C. RMT reveals intrinsic changes to the functional network caused by ADHD

The local properties of the eigenvalues are measured by means of RMT, which separates the system dependent properties of a particular network from the random universal properties of eigenvalues and is thus an effective means of characterizing the intrinsic properties of complex systems [24,29,42]. Since RMT was proposed by Wigner to explain the statistical properties of nuclear spectra [34], widespread applications in various real systems have been

found [15,24,26,28,32,35–38,40–42]. Previous studies have proved that RMT not only predicts the universal behavior of the brain functional network but also accurately characterizes different brain states [29,42]. Thus, RMT was adopted to characterize the abnormalities caused by ADHD in the CF, CC, and MI functional networks. Based on the spectral fluctuations in a complex system, RMT can characterize the correlations among eigenvalues.

1. Insensitivity of the NNSD to ADHD

The NNSD measures the short-range correlations among eigenvalues and has been used to demonstrate universally similar properties of the brain functional network [42]. However, it has been proved that the NNSD is powerless to characterize different brain states [29,42]. Our NNSD results show that the pdfs of the NNSD for the control group and the ADHD group are closer to GOE statistics than to Poisson statistics in the CF, CC, and MI functional networks, revealing a large extent of correlation among the eigenvalues in the brain functional network [29,42]. However, no significant differences in the NNSD were observed between the control group and the ADHD group. Therefore, our results further prove that the NNSD is not an effective means of detecting the abnormalities in the brain functional network caused by ADHD. As proposed in a previous study [29], the reason may be that the short-range correlations among eigenvalues are too strong to be affected by ADHD or other brain states, reflecting the robustness of the brain system to external stimulation.

2. Effective ADHD characterization by means of spectral rigidity and number variance

Both the spectral rigidity and number variance can reflect the long-range correlations among eigenvalues. Many studies have proved that the spectral rigidity and number variance are quite effective for characterizing different brain cognitive states [29,42]. Therefore, the spectral rigidity and number variance should also be considered for characterizing the abnormalities in the brain functional network caused by ADHD. Our results show that the spectral rigidity and number variance exhibit similar behaviors as L varies. At small L, the spectral rigidity and number variance can be predicted by empirical GOE statistics, revealing the universal behavior of the brain functional network. At larger L, they do not follow these predictions but do take the same values in both the control group and the ADHD group, reflecting the properties of the brain functional network that are insensitive to ADHD. At a sufficiently large value of L, the spectral rigidity and number variance in the ADHD group were significantly different from those in the control group, reflecting the specific changes to the functional network caused by ADHD. However, the changes to the spectral rigidity and number variance at sufficiently large L were inconsistent among the CF, CC, and MI functional networks.

First, in the CF functional network, the spectral rigidity and number variance in the ADHD group were obviously smaller than those in the control group. Previous studies have demonstrated that an increase in spectral rigidity and number variance suggests greater randomness of the complex network [24,42]. Therefore, this result indicates that the CF functional network in the ADHD group was more orderly than that in the control group, which suggests that in the resting state, ADHD patients exhibit an abnormality in the CF functional network compared with normal subjects. In general, when normal subjects are performing cognitive tasks, the CF functional connectivity between certain regions is strengthened but is decreased between other regions, which results in greater randomness of the CF functional network [29]. The more orderly CF functional network observed in ADHD patients in the resting state reflects an abnormal increase in CF functional connectivity.

Second, in the CC functional network, the spectral rigidity and number variance in the ADHD group were obviously larger than those in the control group, reflecting greater randomness of the CC functional network in the ADHD group. The association between the activity of one brain region and the activities in other regions as well as the causal sequence of these activities in time are characterized by the corresponding CC. A more random CC functional network indicates greater disorder in causality among different brain regions, which leads to abnormal cooperation among regions in their impact on the activity of a particular region, thereby resulting in abnormality in the functional integration of the brain.

Finally, in the MI functional network, the spectral rigidity and number variance in the ADHD group were again larger than those in the control group, indicating greater randomness of the MI functional network in the ADHD group. In the brain system, one brain region sends information to other regions and obtains feedback from them, and this information flow is measured by the MI. A given region receives integrated information from many other regions. The greater randomness of the MI functional network observed in the ADHD group reflects a more chaotic information flow among different brain regions. Therefore, information integration may be poorly controlled in ADHD patients, leading to a decrease in the global efficiency of the brain, as reported in a previous study [3].

It has to been stressed that the length of eigenvalue for each subject is crucial for the statistical results in RMT. However, the number of brain regions is decided by the brain atlas and it is not unlimited regarding to the practical application of neuroimage technology. Fortunately, similar results were obtained while the brain was divided into 106 regions according to the most commonly used Automated Anatomical Labeling (AAL) atlas [63] (see the Appendix), which further proves the reasonability of our results based on the 444 brain regions. It is also important to note that ADHD induces increased functional connectivity and increases the largest eigenvalue of the brain functional network, which leads to higher synchronization of both the undirected and directed functional networks. However, the CF functional network is more orderly, whereas the CC and MI functional networks are more random. Apparently, the CF is fundamentally different from the CC and MI. Analysis of functional connectivity and the global properties of the eigenvalues are incapable of detecting the differences between the CF functional connectivity

and the CC and MI functional connectivity, but RMT remedies this deficiency. This finding further supports the efficacy of RMT in characterizing the intrinsic properties of the complex brain system. However, a question arises regarding why the levels of randomness differ between the undirected (CF) and directed (CC and MI) functional networks even though they all exhibit a strong degree of synchronization. Currently, the physical mechanism of this phenomenon cannot be explained because of a lack of sufficient evidence, and in the future, this question should be investigated based on extensive simulations.

In summary, we studied the brain functional network in ADHD patients and normal subjects. We first found that ADHD patients exhibit increased undirected and directed functional connectivity as well as stronger synchronization in the brain functional network. Second, we showed that the largest eigenvalue of the brain functional network is increased in ADHD patients. Finally, using RMT, we provided that in ADHD patients, the undirected functional network is more orderly and the directed functional networks are more random compared with those of normal subjects. These findings not only reveal a higher degree of linear dependence, stronger causality, and greater transmission of information in ADHD patients, but also indicate greater disorder in causality and the information flow among brain regions.

ACKNOWLEDGMENTS

We wish to acknowledge the financial support from National Natural Science Foundation of China (Grants No. 11272242, No. 11472202, No. 61473221, No. 61262034, and No. 61462031), Natural Science Foundation of Jiangxi Province (Grant No. 20161ACB21015), Project of the Education Department of Jiangxi Province (Grant No. GJJ150438), and National Basic Research Program of China (Grant No. 2015CB351704).

APPENDIX: RESULTS FOR THE 106 BRAIN REGIONS

In the case that the brain is divided into 106 regions of interest (ROIs) according to the Automated Anatomical Labeling (AAL) atlas [63], the changes caused by ADHD in the functional connectivity (see Fig. 7), the eigenvalue distribution and the largest eigenvalue (see Figs. 8 and 9), and the shot-range and long-range correlation among eigenvalues (see Figs. 10 and 11) are respectively consistent with those for the 444 regions.

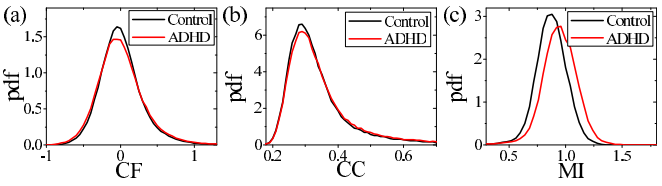

FIG. 7. The pdfs of the (a) CF, (b) CC, and (c) MI for the control group and the ADHD group.

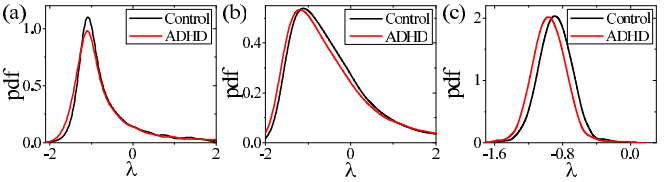

FIG. 8. The pdfs of the eigenvalues for the (a) CF, (b) CC, and (c) MI functional networks in the control group and the ADHD group.

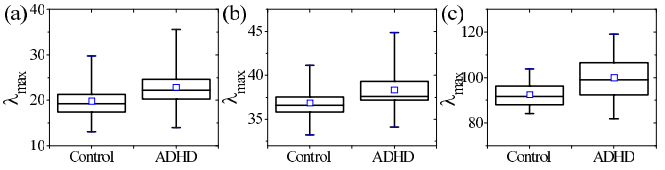

FIG. 9. The box plots of largest eigenvalues for the (a) CF, (b) CC, and (c) MI functional networks in the control group and the ADHD group.

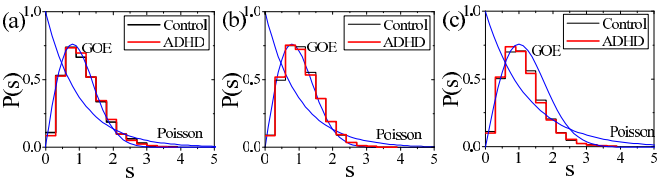

FIG. 10. The probability distributions of the NNSD for the (a) CF, (b) CC, and (c) MI functional networks in the control group and the ADHD group, where the blue lines represent the empirical values predicted by GOE and Poisson statistics.

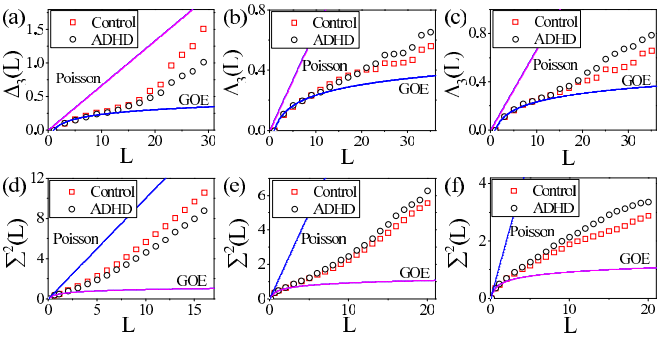

FIG. 11. The spectral rigidity (upper panel) and number variance (lower panel) for the (a) and (d) CF, (b) and (e) CC, and (c) and (f) MI functional networks in the control group and the ADHD group. The blue lines represent the empirical values predicted by GOE and Poisson statistics.

[1] A. De La Fuente, S. Xia, C. Branch, and X. Li, Fron. Hum. Neurosci. **7**, 10422 (2013).
[2] P. H. Wender, Psych. Clin. North Am. **21**, 761 (1998).
[3] P. Lin, J. Sun, G. Yu, Y. Wu, Y. Yang, M. Liang, and X. Liu, Brain Imaging Behav. **8**, 558 (2013).
[4] D. S. Bassett and E. T. Bullmore, Curr. Opin. Neurol. **22**, 340 (2009).
[5] E. Bullmore and O. Sporns, Nat. Rev. Neurosci. **10**, 186 (2009).
[6] O. Sporns, *Networks of the Brain* (MIT, Cambridge, MA, 2011).
[7] J. Gonzalez-Castillo, C. W. Hoy, D. A. Handwerker, M. E. Robinson, L. C. Buchanan, Z. S. Saad, and P. A. Bandettini, Proc. Natl. Acad. Sci. USA **112**, 8762 (2015).
[8] A. Baldassarre, C. M. Lewis, G. Committeri, A. Z. Snyder, G. L. Romani, and M. Corbetta, Proc. Natl. Acad. Sci. USA **109**, 3516 (2012).
[9] K. Konrad and S. B. Eickhoff, Hum. Brain Mapp. **31**, 904 (2010).
[10] F. X. Castellanos and E. Proal, Trends Cogn. Sci. **16**, 17 (2012).
[11] A. Kucyi, M. J. Hove, J. Biederman, K. R. Van Dijk, and E. M. Valera, Hum. Brain Mapp. **36**, 3373 (2015).
[12] J. R. Sato, M. Q. Hoexter, X. F. Castellanos, and L. A. Rohde, PLoS One **7**, e45671 (2012).
[13] S. M. Smith, K. L. Miller, G. Salimi-Khorshidi, M. Webster, C. F. Beckmann, T. E. Nichols, J. D. Ramsey, and M. W. Woolrich, Neuroimage **54**, 875 (2011).
[14] F. Ren and W.-X. Zhou, PLoS One **9**, e97711 (2014).
[15] V. Plerou, P. Gopikrishnan, B. Rosenow, L. A. Nunes Amaral, and H. E. Stanley, Phys. Rev. Lett. **83**, 1471 (1999).
[16] J. Jeong, J. C. Gore, and B. S. Peterson, Clin. Neurophysiol. **112**, 827 (2001).
[17] S. Bialonski and K. Lehnertz, Chaos **23**, 033139 (2013).
[18] P. Lin, Y. Yang, J. Jovicich, N. De Pisapia, X. Wang, C. S. Zuo, and J. J. Levitt, Brain Imaging Behav. **10**, 212 (2016).
[19] C. Stam, B. Jones, G. Nolte, M. Breakspear, and P. Scheltens, Cereb. Cortex **17**, 92 (2007).
[20] R. Wang, P. Lin, and Y. Wu, *Exploring Dynamic Temporal-topological Structure of Brain Network within ADHD* (Springer, Netherlands, Dordrecht, 2015), pp. 93–98.
[21] L. Tian, T. Jiang, Y. Wang, Y. Zang, Y. He, M. Liang, M. Sui, Q. Cao, S. Hu, M. Peng, and Y. Zhuo, Neurosci. Lett. **400**, 39 (2006).
[22] X. H. Wang and L. Li, Eur. J. Radiol. **84**, 947 (2015).
[23] R. Wang, J. Li, L. Wang, Y. Yang, P. Lin, and Y. Wu, Physica A **463**, 219 (2016).
[24] J. N. Bandyopadhyay and S. Jalan, Phys. Rev. E **76**, 026109 (2007).
[25] J. L. Gross and J. Yellen, *Handbook of Graph Theory* (CRC, Boca Raton, Florida, 2004).
[26] V. Plerou, P. Gopikrishnan, B. Rosenow, L. A. Nunes Amaral, T. Guhr, and H. E. Stanley, Phys. Rev. E **65**, 066126 (2002).
[27] M. C. Munnix, T. Shimada, R. Schafer, F. Leyvraz, T. H. Seligman, T. Guhr, and H. E. Stanley, Sci. Rep. **2**, 644 (2012).
[28] H. Meng, W. J. Xie, Z. Q. Jiang, B. Podobnik, W. X. Zhou, and H. E. Stanley, Sci. Rep. **4**, 3655 (2014).
[29] R. Wang, Z.-Z. Zhang, J. Ma, Y. Yang, P. Lin, and Y. Wu, Chaos **25**, 123112 (2015).
[30] J. G. Restrepo, E. Ott, and B. R. Hunt, Phys. Rev. Lett. **97**, 094102 (2006).
[31] J. G. Restrepo, E. Ott, and B. R. Hunt, Phys. Rev. E **76**, 036151 (2007).
[32] S. Jalan and J. N. Bandyopadhyay, Europhys. Lett. **87**, 48010 (2009).
[33] S. Jalan, N. Solymosi, G. Vattay, and B. Li, Phys. Rev. E **81**, 046118 (2010).
[34] E. P. Wigner, *Characteristic Vectors of Bordered Matrices with Infinite Dimensions I* (Springer, Berlin, Heidelberg, 1993), pp. 524–540.
[35] M. S. Santhanam and P. K. Patra, Phys. Rev. E **64**, 016102 (2001).
[36] S. M. Gibson, S. P. Ficklin, S. Isaacson, F. Luo, F. A. Feltus, and M. C. Smith, PLoS One **8**, e55871 (2013).
[37] I. Osorio and Y. C. Lai, Chaos **21**, 033108 (2011).
[38] F. Luo, Y. Yang, J. Zhong, H. Gao, L. Khan, D. K. Thompson, and J. Zhou, BMC Bioinformatics **8**, 299 (2007).
[39] T. Kottos and U. Smilansky, Phys. Rev. Lett. **79**, 4794 (1997).
[40] S. Jalan and J. N. Bandyopadhyay, Physica A **387**, 667 (2008).
[41] D. Mulhall, Phys. Rev. C **91**, 014305 (2015).
[42] P. Seba, Phys. Rev. Lett. **91**, 198104 (2003).
[43] http://fcon_1000.projects.nitrc.org/.
[44] http://afni.nimh.nih.gov/afni/.
[45] R. W. Cox, Comput. Biomed. Res. **29**, 162 (1996).
[46] http://www.fmrib.ox.ac.uk/fsl/.
[47] A. Abraham, F. Pedregosa, M. Eickenberg, P. Gervais, A. Mueller, J. Kossaifi, A. Gramfort, B. Thirion, and G. Varoquaux, Front. Neuroinform. **8**, 1 (2014).
[48] Z. Zhang, S. Sun, M. Yi, X. Wu, and Y. Ding, Biomed. Res. Int. **2015**, 825136 (2015).
[49] H. Peng, F. Long, and C. Ding, IEEE T. Pattern. Anal. **27**, 1226 (2005).
[50] R. A. Fisher, Biometrika **10**, 507 (1915).
[51] S. Jalan, C. Sarkar, A. Madhusudanan, and S. K. Dwivedi, PLoS ONE **9**, 1 (2014).
[52] S. Jalan, Pramana J. Phys. **84**, 285 (2015).
[53] W. Luo and P. Sarnak, Commun. Math. Phys. **161**, 419 (1994).
[54] C. J. Honey, R. Kotter, M. Breakspear, and O. Sporns, Proc. Natl. Acad. Sci. USA **104**, 10240 (2007).
[55] J. Hlinka, M. Palus, M. Vejmelka, D. Mantini, and M. Corbetta, Neuroimage **54**, 2218 (2011).
[56] T. Conlon, H. J. Ruskin, and M. Crane, Physica A **388**, 705 (2009).
[57] D. Hartman, J. Hlinka, M. Palus, D. Mantini, and M. Corbetta, Chaos **21**, 013119 (2011).
[58] D. A. P. Association, *Diagnostic and Statistical Manual of Mental Disorders*, 5th ed. (American Psychiatric Publishing, Arlington, 2013).
[59] F. X. Castellanos, D. S. Margulies, C. Kelly, L. Q. Uddin, M. Ghaffari *et al.*, Biol. Psychiat. **63**, 332 (2008).
[60] C. Zhou, L. Zemanová, G. Zamora-López, C. C. Hilgetag, and J. Kurths, New J. Phys. **9**, 178 (2007).
[61] P. Kudela, P. J. Franaszczuk, and G. K. Bergey, Biol. Cybern. **88**, 276 (2003).
[62] I. Jolliffe, *Principal Component Analysis*, 2nd ed. (Springer, New York, 2002).
[63] N. Tzourio-Mazoyer, B. Landeau, D. Papathanassiou, F. Crivello, O. Etard, N. Delcroix, B. Mazoyer, and M. Joliot, Neuroimage **15**, 273 (2002).